E-ISSN: 2948-5231
Article
Journal of Asian Geography, 2026, Volume 5 (Issue 2), 25-33
https://doi.org/10.36777/jag2026.5.2.3



# GIS-Based Landslide Risk Screening in Segamat, Johor, with Historical Earthquake Context

Wang Huijin[1], Ismail Ahmad Abir[2], Mohd Amirul Mahamud[1,*]

[1] Geography Section, School of Humanities, Universiti Sains Malaysia, 11800 USM, Penang, Malaysia.
[2] School of Physics, Universiti Sains Malaysia, 11800 USM, Penang, Malaysia.

*Correspondence: mohd.amirul@usm.my

Received: 26 May 2026, Revised: 26 Aug 2026; Accepted: 29 Aug 2026; Published 29 Sep 2026

**Abstract**: Landslide assessment in humid tropical, low-seismicity regions requires a clear distinction between terrain susceptibility and the consequences associated with exposed populations and infrastructure. This study develops a geographic information system (GIS)-based screening framework for Segamat, Johor, by integrating physical susceptibility, exposure, and vulnerability through multi-criteria decision analysis and the Analytic Hierarchy Process (AHP). Nine physical indicators, ten exposure indicators, and six vulnerability indicators were standardised into five ordinal classes and combined using weighted overlay. The three component surfaces were then multiplied to produce a relative landslide-risk index. High and very high physical susceptibility were concentrated in eastern and south-eastern Segamat, where steeper slopes, greater rainfall, dense lineaments, and proximity to rivers coincide. Exposure was more localised around settlement and service centres, while vulnerability increased in areas with larger concentrations of dependent population groups and poorer access to emergency and health facilities. The integrated map identified priority clusters around Kampung Abdullah and Taman Tan Leng Ann, together with isolated patches in eastern Segamat that warrant field verification. A supplementary co-location analysis found that moderate-to-very-high susceptibility occupied 53.3%, 46.0%, and 51.7% of nested 5, 15, and 25 km earthquake buffers, respectively. Because the susceptibility model contains no ground-motion variable and the buffers are nested, these percentages do not establish earthquake triggering or attenuation. The output is therefore best interpreted as a regional screening tool for directing landslide inventories, geotechnical investigations, development review, and preparedness, rather than as a probabilistic hazard forecast or parcel-level stability assessment.

**Keywords**: Analytic hierarchy process; historical seismicity; landslide susceptibility; multi-criteria decision analysis; Segamat

## 1.0 Introduction

Landslides emerge from the interaction of terrain, material properties, water and human disturbance. In humid tropical settings, deep weathering and intense or prolonged rainfall can raise pore-water pressure, reduce effective stress and mobilise unstable slope material (Crozier, 2010). Steep slopes, weak or fractured lithology, drainage incision and road cuts may intensify these processes. Where settlements and infrastructure occupy susceptible terrain, a local slope failure can become a serious social and economic disruption. Effective assessment must therefore distinguish the physical propensity for landsliding from exposure and vulnerability, which shape the consequences of an event (Fell et al., 2008; Van Westen et al., 2006).

Regional susceptibility mapping is useful where detailed geotechnical measurements and complete event inventories are unavailable. Geographic information systems (GIS) allow diverse conditioning factors to be aligned and compared, while multi-criteria decision analysis (MCDA) provides an explicit framework for combining evidence and expert judgement (Malczewski, 2006). The Analytic Hierarchy Process (AHP) is widely used for this purpose because it structures the relative importance assigned to each criterion (Saaty, 1980). Applications in Malaysia and elsewhere have shown that GIS-AHP can identify plausible spatial patterns of landslide susceptibility, particularly in data-constrained regions (Lee & Pradhan, 2007; Shahabi & Hashim, 2015). The method is transparent and readily transferable, but its outputs remain sensitive to factor selection, class boundaries and subjective weights. They should not be interpreted as probabilities unless calibrated against a suitable inventory (Reichenbach et al., 2018).

Peninsular Malaysia is commonly described as a comparatively stable part of the Sundaland block, yet it is not entirely aseismic. Historical macroseismic evidence indicates that two moderate intraplate earthquakes occurred in the peninsula in 1922, with reassessed local magnitudes of approximately 5.4 and 5.0 (Martin et al., 2020). On 24 August 2025, the Malaysian Meteorological Department reported a magnitude 4.1 earthquake approximately 5 km west of Segamat at a depth of about 10 km, followed by smaller events in the wider area (Malaysian Meteorological Department, 2025). These observations justify renewed attention to seismic context in local geohazard studies. They do not, by themselves, show that mapped landslides were earthquake-induced.

This distinction is important. Earthquake-triggered landslides are controlled by shaking intensity, magnitude, depth, source distance, topography and material properties, and their attribution requires temporally linked landslide observations (Keefer, 1984). A susceptibility model built from static environmental variables cannot isolate the influence of shaking if no peak ground acceleration, intensity or event-specific variable is included. Proximity buffers around epicentres can describe spatial co-location, but they cannot substitute for a ground-motion model or establish causality. This study therefore treats the 1922 and 2025 earthquakes as historical context and evaluates only whether elevated terrain susceptibility occurs near selected epicentres.

Against this background, the study develops a relative landslide-risk screening map for Segamat District, Johor. Its objectives are to (1) integrate topographic, geological, hydrological and land-cover factors into a physical susceptibility surface; (2) map exposure and vulnerability using demographic, built-environment and accessibility indicators; (3) combine the three components to locate priority screening areas; and (4) examine the spatial composition of susceptibility classes within nested earthquake buffers. The contribution is a transparent first-pass framework for targeting field inventories, slope investigation and planning attention in a tropical district where both landslide and seismic records remain limited.

## 2.0 Study Area

Segamat occupies northern Johor in southern Peninsular Malaysia (Figure 1). The district includes a western lowland and settlement corridor, an undulating interior, and more rugged terrain towards the east and south-east. The eastern landscape extends towards the Endau-Rompin forest complex. Segamat town and its surrounding neighbourhoods form the principal concentration of population, buildings and services, while smaller settlements and transport routes are dispersed across the district.

The climate is humid tropical and strongly influenced by monsoonal circulation. Frequent rainfall sustains weathering and high soil moisture, while prolonged or intense episodes can destabilise slopes that are already steep, fractured or modified. Geological structure is locally

Article Journal of Asian Geography, 2026, Volume 5 (Issue 2), 25-33
https://doi.org/10.36777/jag2026.5.2.3
E-ISSN: 2948-5231


expressed by mapped lithological variation and lineaments, and drainage channels can promote saturation or toe erosion. Road construction, land-cover conversion and settlement growth add local disturbances to this environmental setting.

From a seismic perspective, Segamat lies within a low-activity intraplate region rather than an active plate boundary. Regional earthquakes generated around Sumatra may be felt in Peninsular Malaysia, and rare local events have also occurred within the peninsula (Nazaruddin & Duerrast, 2021; Simons et al., 2007). The selected historical and recent epicentres shown in Figure 1 provide the basis for the supplementary buffer analysis. Their inclusion is contextual: the physical susceptibility model itself does not contain an earthquake-shaking layer.

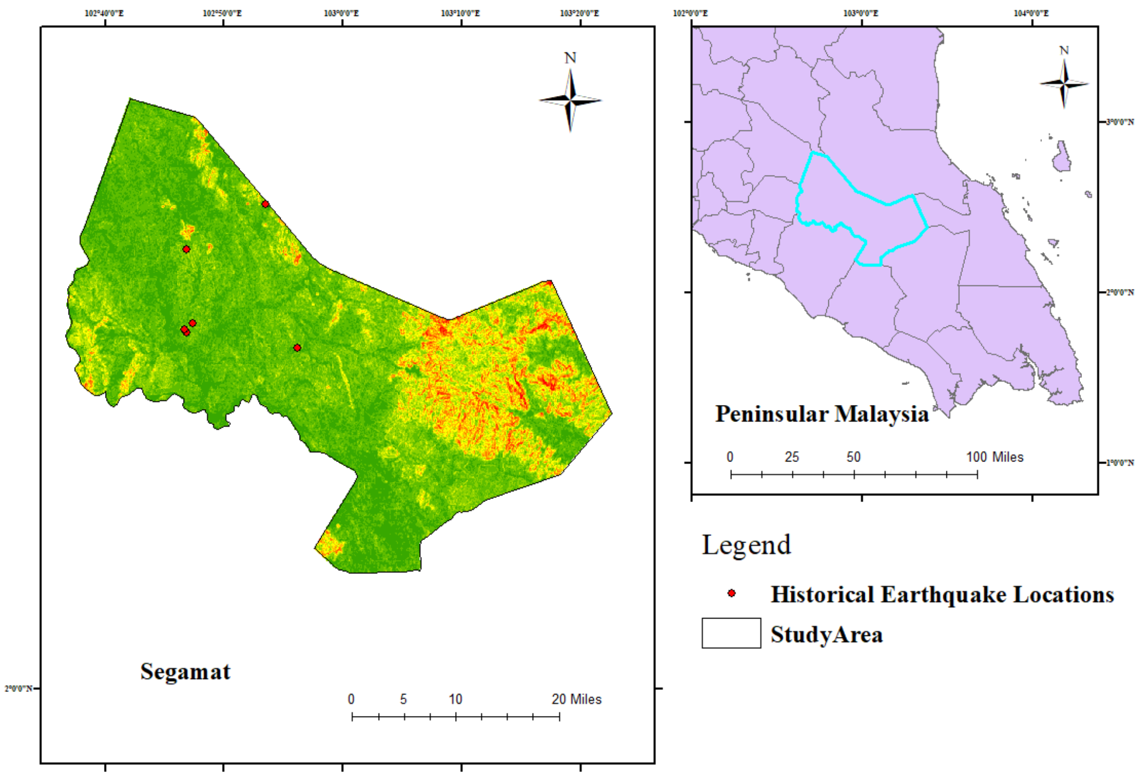


Figure 1: Segamat study area and the historical and recent earthquake locations considered in the spatial-context analysis.

## 3.0 Materials and Methodology

### *3.1 Analytical framework and data*

Risk was represented as the spatial conjunction of physical susceptibility, exposure and vulnerability. Physical susceptibility describes the relative propensity of terrain to fail, given the conditioning factors represented in the model. Exposure denotes people, buildings, commercial functions and public assets that may be affected. Vulnerability represents demographic sensitivity and limitations in access or response capacity. The analysis does not estimate landslide frequency, runout, volume, velocity or expected loss.

The workflow comprised data acquisition, spatial preprocessing, factor standardisation, AHP weighting, component overlay, risk integration and spatial-context checks. All layers were projected, clipped to the district boundary and converted to a common raster framework. A 30 m Shuttle Radar Topography Mission digital elevation model (DEM) provided the terrain base (Farr et al., 2007). Slope, aspect and elevation were derived from the DEM. Lineaments were extracted from the terrain data using automated image-processing tools and converted to a line-density surface. Lithology was obtained from Geological Survey of Malaysia mapping, and land use and land cover (LULC) were represented by ESA WorldCover (Zanaga et al., 2022).

Rainfall was obtained from the Climatic Research Unit Time-Series dataset and interpolated to create a continuous district surface (Harris et al., 2020). The source product has a 0.5-degree grid, so resampling it to the analysis grid aligns cells but does not create fine-scale rainfall information. River and transport proximity were calculated as Euclidean-distance rasters from mapped networks. OpenStreetMap supplied roads and multiple categories of buildings and facilities, while WorldPop supplied population and demographic surfaces (OpenStreetMap contributors, 2025; Tatem, 2017). The source thesis did not consistently record the edition, acquisition date or native resolution of every vector layer; Table 1 therefore reports only details that can be supported from the documented workflow.

Twenty-five indicators were organised into three components (Table 1). The physical component used nine factors. The exposure component represented the density of buildings, general population, commercial activities, financial services, government facilities, public facilities, water-related facilities, other mapped facilities, men and youth. The vulnerability component represented older people, children, women, distance to emergency services, distance to health facilities and road density. Demographic and facility variables serve different analytical roles: exposure measures what is located in potentially affected areas, whereas vulnerability represents characteristics that may constrain evacuation, access or recovery.

E-ISSN: 2948-5231
Article Journal of Asian Geography, 2026, Volume 5 (Issue 2), 25-33
https://doi.org/10.36777/jag2026.5.2.3


Table 1: Indicators, data sources or derivations, and AHP weights used in the three model components.

| Component | Indicator | Data source or derivation | AHP weight |
|---|---|---|---|
| Physical susceptibility | Slope | Derived from SRTM DEM | 0.226 |
| Physical susceptibility | Rainfall | CRU TS precipitation; IDW interpolation | 0.182 |
| Physical susceptibility | Lithology | Geological Survey of Malaysia mapping | 0.146 |
| Physical susceptibility | Lineament density | Lineaments extracted from DEM; GIS density | 0.116 |
| Physical susceptibility | Distance to river | Mapped drainage; Euclidean distance | 0.102 |
| Physical susceptibility | LULC | ESA WorldCover | 0.088 |
| Physical susceptibility | Elevation | SRTM DEM | 0.063 |
| Physical susceptibility | Distance to transport | OpenStreetMap network; Euclidean distance | 0.049 |
| Physical susceptibility | Aspect | Derived from SRTM DEM | 0.028 |
| Exposure | Building density | OpenStreetMap building data; density surface | 0.189 |
| Exposure | General population density | WorldPop population surface | 0.189 |
| Exposure | Commercial density | OpenStreetMap facilities; density surface | 0.128 |
| Exposure | Financial-facility density | OpenStreetMap facilities; density surface | 0.098 |
| Exposure | Government-facility density | OpenStreetMap facilities; density surface | 0.081 |
| Exposure | Public-facility density | OpenStreetMap facilities; density surface | 0.074 |
| Exposure | Water-facility density | OpenStreetMap facilities; density surface | 0.074 |
| Exposure | Other facility density | Mapped facility locations; density surface | 0.070 |
| Exposure | Men density | WorldPop demographic surface | 0.055 |
| Exposure | Youth density | WorldPop demographic surface | 0.042 |
| Vulnerability | Older-people density | WorldPop demographic surface | 0.284 |
| Vulnerability | Children density | WorldPop demographic surface | 0.219 |
| Vulnerability | Women density | WorldPop demographic surface | 0.161 |
| Vulnerability | Distance to emergency services | OpenStreetMap facilities; Euclidean distance | 0.139 |
| Vulnerability | Distance to health facilities | OpenStreetMap facilities; Euclidean distance | 0.114 |
| Vulnerability | Road density | OpenStreetMap road network; density surface | 0.083 |

### *3.2 Standardisation and AHP weighting*

Continuous layers were converted to comparable ordinal scores from 1 (very low) to 5 (very high). Jenks natural breaks were used to identify five classes within each layer. Higher slope, rainfall and lineament density received progressively higher physical scores, while locations nearer rivers and transport corridors received higher scores because of possible toe erosion, saturation, slope cutting and drainage disturbance. Lithology and LULC were ranked by their interpreted relative contribution to slope instability. Density and accessibility variables were assigned in the direction implied by their component; for example, a high building density increased exposure, while a long distance from emergency or health facilities increased vulnerability.

AHP weights were applied separately within each component. In a conventional AHP procedure, reciprocal pairwise comparisons are used to derive a normalised priority vector, and judgement consistency is evaluated through the consistency ratio (Saaty, 1980). The final weights documented for this study each sum to 1.000 within their component. Slope (0.226), rainfall (0.182) and lithology (0.146) dominate the physical index. Building density and general population density share the highest exposure weight (0.189 each). Older people (0.284), children (0.219) and women (0.161) collectively account for 66.4% of the vulnerability index.

For component d, the standardised index was calculated as:

$$I\_d = \Sigma(w\_di \times s\_di)$$

where $w\_di$ is the AHP weight of indicator i and $s\_di$ is its ordinal score. Each resulting surface was reclassified into very low, low, moderate, high and very high classes using natural breaks. Although the source workflow states that consistency was checked, the pairwise matrices, maximum eigenvalues and numerical consistency ratios were not reported. The final weights can therefore be reproduced, but the underlying judgements cannot be independently audited from the available documentation.

E-ISSN: 2948-5231
Article Journal of Asian Geography, 2026, Volume 5 (Issue 2), 25-33
https://doi.org/10.36777/jag2026.5.2.3

*3.3 Integrated landslide-risk index*

The physical, exposure and vulnerability surfaces were combined using the multiplicative relationship documented in the analytical workflow:

$$R = S \times E \times V$$

where R is the relative risk index, S is physical susceptibility, E is exposure and V is vulnerability. Multiplication preserves the conditional logic that high risk requires the spatial concurrence of all three components. It also makes the output sensitive to the scale and lower bound of each component, which is why all three were first expressed on the same five-level ordinal scale. The product was divided into five relative classes using Jenks natural breaks. These classes rank locations within Segamat; they do not express an annual probability or an absolute risk threshold and should not be compared directly with classes derived for a different study area.

*3.4 Landslide overlay and earthquake-buffer analysis*

A small, non-exhaustive set of historical landslide locations was overlaid on the susceptibility and risk maps as a qualitative plausibility check. The source inventory was insufficient for data partitioning or statistical validation. No receiver operating characteristic curve, area under the curve, success-rate curve or independent event-based test was therefore calculated. The overlay was used only to inspect whether mapped points occurred in terrain that the model represented as comparatively susceptible.

Historical and recent earthquake epicentres were also overlaid. Nested buffers of 5, 15 and 25 km were generated around the selected locations, and a zonal histogram measured the proportion of each buffer occupied by susceptibility classes. To summarise the upper part of the susceptibility distribution, the moderate, high and very high classes were combined:

$$P\_r = (A\_moderate + A\_high + A\_very\ high) / A\_r \times 100$$

where P_r is the share of moderate-to-very-high susceptibility in the buffer of radius r, the numerator is the combined area of those classes and A_r is the total analysed buffer area. Because the buffers are cumulative and nested, the 15 and 25 km values include the inner areas. Differences among radii consequently reflect the composition of progressively larger landscapes, not independent distance bands. Without ground-motion measures and landslide dates, this analysis can demonstrate only spatial co-location.

**4.0 Results**

*4.1 Physical susceptibility pattern*

The physical component showed a pronounced east-west contrast (Figure 2a). High and very high values were concentrated mainly in eastern and south-eastern Segamat, where steep or rugged terrain coincided with comparatively high rainfall, dense lineaments and proximity to river channels. Slope and rainfall together contributed 40.8% of the physical weight, while lithology and lineament density contributed a further 26.2%. The resulting pattern therefore reflects a strong topographic, hydrological and structural control. Low and very low values were more extensive in the western part of the district, where relief is gentler and the weighted physical conditions were comparatively less favourable to slope failure.

The five-class susceptibility surface retained this broad contrast (Figure 2d). Moderate susceptibility occupied much of the transitional terrain, whereas the upper classes formed more discontinuous belts and patches in the east and south-east. Proximity to roads and disturbed LULC locally raised susceptibility, but their weights were smaller than those of slope, rainfall and lithology. The qualitative landslide overlay indicated that the available points were generally situated in moderate-to-high terrain, although the inventory is too small and incompletely documented to quantify predictive skill.

*4.2 Exposure and vulnerability*

Exposure was spatially concentrated around settlement and service clusters rather than distributed continuously across the district (Figure 2b). Most peripheral and forested areas had very low or low exposure. Higher values occurred where buildings, general population and commercial or public functions converged. Building density and general population density together accounted for 37.8% of the exposure weight, so established settlement centres exerted the strongest influence on the component. Commercial density contributed another 12.8%, while financial, government, public, water-related and other facilities differentiated smaller functional centres.

Vulnerability followed a different geography (Figure 2c). Higher values extended through parts of the north and east and in peripheral locations where dependent population groups coincided with longer distances to emergency or health services. Older people, children and women jointly carried 66.4% of the vulnerability weight, while the two service-distance indicators contributed 25.3%. Road density supplied the remaining 8.3%. These variables provide useful screening proxies, but they do not directly measure household income, disability, housing quality, vehicle access, social support or institutional response capacity.

E-ISSN: 2948-5231
Article
Journal of Asian Geography, 2026, Volume 5 (Issue 2), 25-33
https://doi.org/10.36777/jag2026.5.2.3

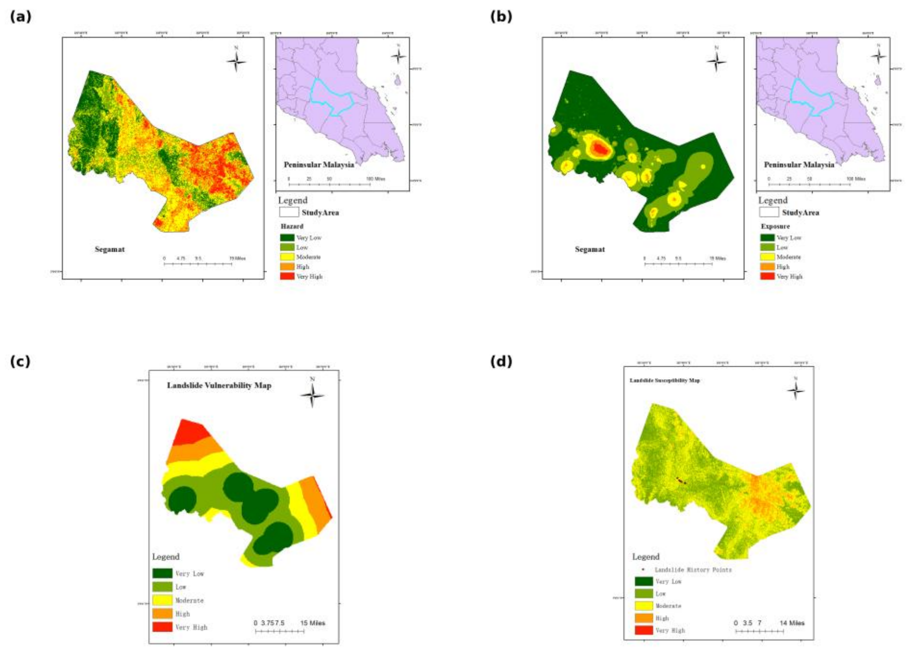


Figure 2: Spatial distribution of (a) the weighted physical component (labelled "Hazard" in the source GIS output), (b) exposure, (c) vulnerability and (d) five-class susceptibility with the available historical landslide points.

*4.3 Integrated risk pattern*

The integrated map produced a more selective pattern than the physical surface alone (Figure 3). Priority clusters occurred around Kampung Abdullah and Taman Tan Leng Ann, where susceptible terrain overlapped with relatively dense population, buildings, infrastructure and limited access represented in the vulnerability indicators. These locations are the clearest candidates for field reconnaissance, inventory improvement and site-level slope assessment.

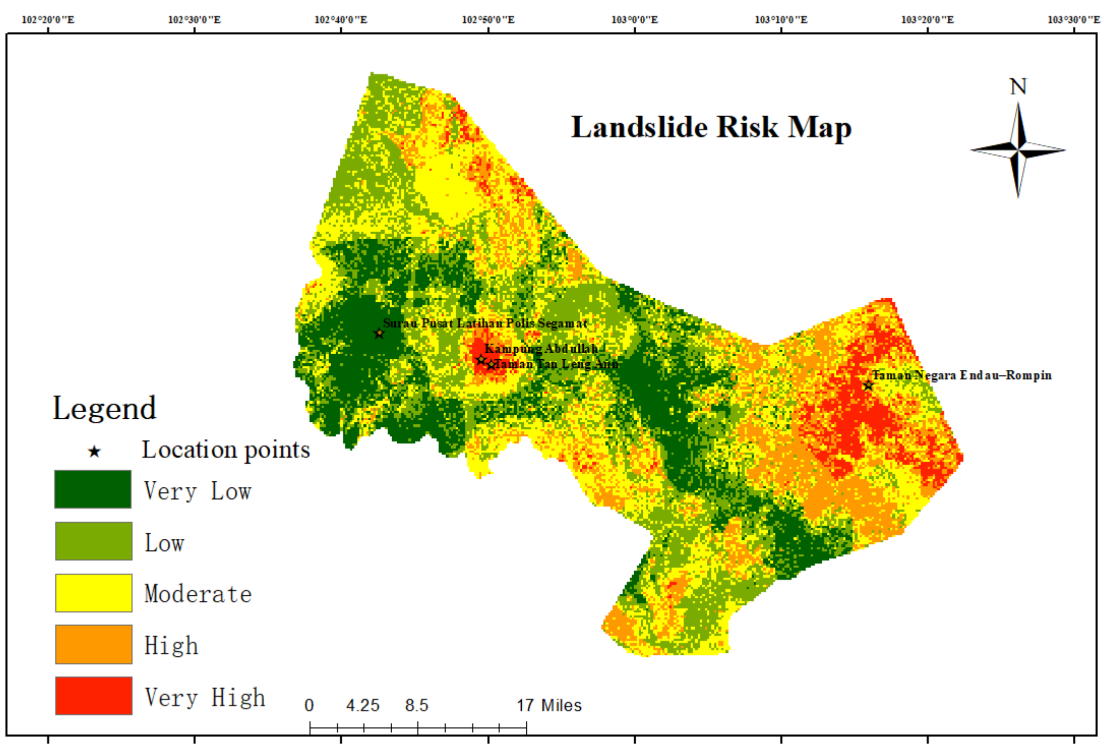


Figure 3: Relative landslide-risk classes produced by multiplying the physical susceptibility, exposure and vulnerability indices.

E-ISSN: 2948-5231
Article
Journal of Asian Geography, 2026, Volume 5 (Issue 2), 25-33
https://doi.org/10.36777/jag2026.5.2.3

Isolated high and very high classes also appeared in the eastern district, including parts of the landscape towards Taman Negara Endau-Rompin. Their interpretation requires particular care. Exposure is relatively sparse in much of this terrain, and the multiplicative index can still produce a high class where physical susceptibility is extreme and the other components are above their local lower bounds. A high map class in a remote area does not imply the same potential losses as a densely settled hotspot. The underlying component values should therefore be consulted whenever a site is prioritised.

Very low and low risk was more common across gently sloping western areas with comparatively limited physical susceptibility or lower combined exposure and vulnerability. The contrast between the component maps and final risk map illustrates why susceptibility and risk should not be used interchangeably: a physically unstable slope with no people or assets nearby may be a geomorphic concern but not a high social-risk location, whereas moderately susceptible terrain can become a planning priority when exposure and vulnerability are substantial.

*4.4 Integrated risk pattern*

Moderate-to-very-high susceptibility occupied 53.3% of the area within the nested 5 km buffers, 46.0% within 15 km and 51.7% within 25 km (Table 2; Figure 4). The 5 km value confirms that a substantial amount of comparatively susceptible terrain lies near selected epicentres. The fall at 15 km and subsequent rise at 25 km is non-monotonic, however. It does not support a simple attenuation interpretation in which susceptibility steadily decreases with distance.

Table 2: Share of moderate-to-very-high landslide susceptibility within nested earthquake buffers.

| Buffer radius (km) | Moderate-to-very-high susceptibility (%) | Interpretive note |
|---|---|---|
| 5 | 53.3 | Cumulative area within 5 km |
| 15 | 46.0 | Includes the 5 km area |
| 25 | 51.7 | Includes the 5 and 15 km areas |

The 25 km buffers encompass more of the eastern and south-eastern terrain where slope, rainfall, lineaments and drainage already produce high physical scores. The larger percentage at 25 km can therefore be explained by changing landscape composition without invoking a persistent seismic effect. Likewise, the 5 km percentage cannot be attributed to shaking because the susceptibility layer is independent of earthquake magnitude, depth, intensity and event date. The result is evidence of spatial coincidence only.

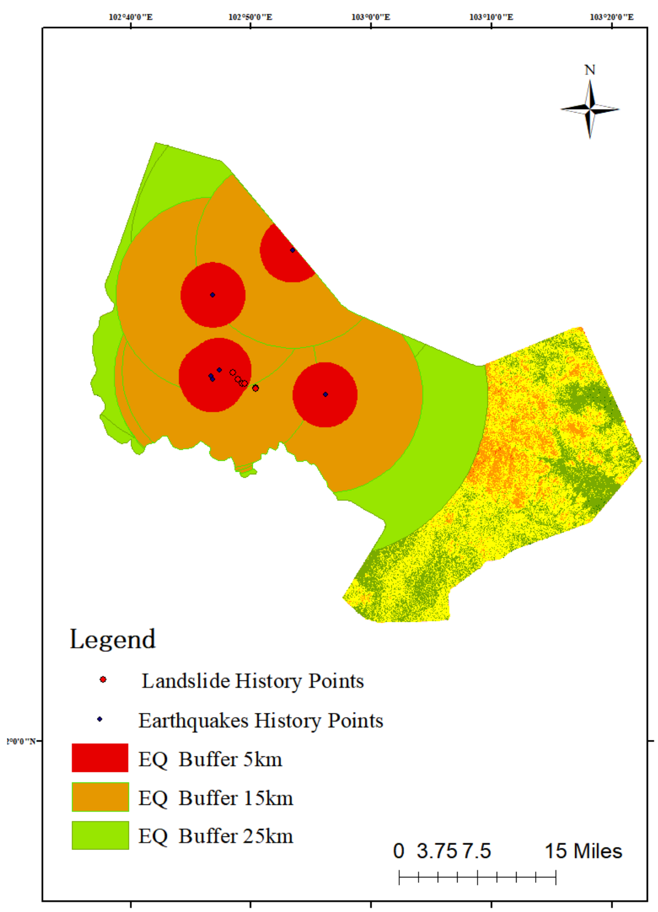


Figure 4: Nested 5, 15 and 25 km buffers around selected earthquake epicentres overlaid on landslide susceptibility classes.

Journal of Asian Geography, 2026, Volume 5 (Issue 2), 25-33
https://doi.org/10.36777/jag2026.5.2.3
E-ISSN: 2948-5231

## 5.0 Discussion

### *5.1 Environmental and social controls on mapped risk*

The eastern concentration of physical susceptibility is consistent with established landslide controls. Slope increases the downslope component of gravity, fractured lithology and lineaments reduce material continuity, and rainfall promotes saturation and loss of effective strength. Rivers can undercut toes or concentrate moisture, while roads alter slope geometry and drainage. Comparable interactions have been documented in tropical and earthquake-affected mountain regions (Chigira et al., 2010; Dai et al., 2011). The Segamat map expresses these mechanisms as a relative index rather than measuring factor-response relationships directly.

The shift from a broad susceptibility surface to localised risk clusters is analytically important. Exposure is dominated by buildings and population, while vulnerability gives greatest weight to dependent demographic groups and service accessibility. Kampung Abdullah and Taman Tan Leng Ann are prioritised because multiple components coincide, not because any single physical factor is extreme everywhere within them. This component-based interpretation is more useful for planning than a single composite colour. It allows a response to match the local driver: slope drainage and stabilisation where physical susceptibility dominates, development control where exposure is increasing, or emergency-access improvement where vulnerability is elevated.

The vulnerability indicators nevertheless require cautious social interpretation. Women, children and older people are heterogeneous groups, and demographic status alone does not determine disaster capacity. Road density can either support access or indicate development pressure, depending on its location and condition. Facility proximity does not measure staffing, capacity, opening hours or travel time during heavy rainfall. Future work should combine these proxies with locally collected data on disability, income, housing, vehicle availability, warning access and social networks. Participatory weighting with district agencies and residents would also make the vulnerability model more context-sensitive (Birkmann, 2013).

### *5.2 What the seismic context does and does not show*

The earthquake record changes how geohazards in Segamat should be discussed, but it does not change what the present model measures. The 1922 events establish that rare moderate intraplate earthquakes have occurred in Peninsular Malaysia (Martin et al., 2020), and the 2025 sequence confirms that small local events remain possible. Ground shaking can trigger landslides when acceleration and duration exceed thresholds conditioned by slope and material properties (Keefer, 1984). Demonstrating that process for Segamat would require event-specific shaking estimates and a landslide inventory dated closely enough to distinguish co-seismic failures from rainfall-induced or construction-related events.

The nested-buffer results do not meet that evidential standard. First, the susceptibility index contains no seismic variable, so its spatial pattern cannot be a modelled response to shaking. Second, epicentral distance is an incomplete proxy for shaking because magnitude, depth, rupture geometry, path effects and local amplification matter. Third, cumulative buffers are not independent rings. The non-monotonic percentages—53.3%, 46.0% and 51.7%—mainly show that the terrain mixture changes as the analysis expands outward. Finally, the timing of the landslide points was not linked to the earthquakes. Describing the result as co-location prevents an ecologically plausible association from being mistaken for causal evidence.

A stronger seismic-landslide assessment should generate peak ground acceleration or macroseismic intensity surfaces for defined events, include distance to mapped active or potentially active structures, and match landslide occurrence dates to shaking and rainfall. Event-based inventories derived from optical or radar satellite imagery could be compared before and after an earthquake. Statistical or physically based models could then test whether shaking adds explanatory power beyond slope, lithology, rainfall and land cover. Until these data exist, the earthquake overlay is best used to identify places where post-event reconnaissance may be especially valuable.

### *5.3 Planning implications*

The map provides a practical sequence for risk reduction. At the district scale, high and very high classes can guide reconnaissance and the creation of a standardised landslide inventory. For settled hotspots, field teams should inspect cut slopes, retaining structures, drainage outlets, signs of creep, tension cracks and past repairs. Planning authorities can use the component maps to flag development applications that require geotechnical investigation, but approval or rejection should never rest on this regional raster alone.

Risk reduction should reflect the source of the mapped score. In physically susceptible corridors, priority measures include surface and subsurface drainage maintenance, erosion control, vegetation management and engineered stabilisation were obtained by site investigation. Where exposure is rising, setbacks, development controls and protection of drainage paths can prevent avoidable increases in risk. In vulnerable communities, emergency-route redundancy, accessible warning communication and response planning may reduce consequences even when the underlying slope cannot readily be altered.

Monitoring should also recognise that rainfall remains the most credible frequent trigger in this humid tropical environment. Rain gauges, soil-moisture sensors, crack gauges and low-cost displacement instruments could be installed at verified active or marginal slopes, with thresholds calibrated against local observations. After felt earthquakes, targeted inspections of already susceptible slopes would be prudent, especially following or during wet periods. Such inspections are a precautionary response to compound conditions, not evidence that a specific earthquake has destabilised a slope.

### *5.4 Methodological uncertainty and limitations*

Several limitations constrain the map's precision and explanatory strength. The source datasets have different dates, scales and positional accuracies. In particular, CRU TS rainfall is distributed on a 0.5-degree grid (Harris et al., 2020), much coarser than the 30 m terrain grid. Interpolation and resampling cannot recover local rainfall gradients absent from the source. The editions and acquisition dates of some road, river, facility, geological and demographic layers were not fully documented, which limits exact replication and may introduce temporal mismatch.

AHP weights are judgement-based. Although the final weights sum correctly within each component, the pairwise matrices and numerical consistency ratios were unavailable, preventing independent assessment of judgement consistency. No formal sensitivity analysis was reported. Given the strong weights assigned to slope, rainfall, dependent population groups and settlement density, modest changes to these priorities could alter class boundaries and hotspot locations. Future analyses should publish all matrices, justify each comparison, report consistency statistics and test rank stability across plausible weight sets.

The five-class natural-break scheme is relative to the empirical distribution in Segamat. Class thresholds may shift if the study boundary, input period or dataset is changed. The multiplicative risk formulation is also sensitive to input scaling and can elevate remote cells when one component is extreme and the others are non-zero. Reporting continuous component values alongside classes and comparing multiplicative, additive and fuzzy formulations would clarify this sensitivity.

Validation is the most important data gap. The available landslide inventory was small, non-exhaustive and not sufficiently documented for statistical testing. A visual overlay cannot quantify false positives, false negatives or spatial calibration. The map also omits landslide type, initiation-versus-runout zones, failure volume, temporal probability and event magnitude. A systematic multi-temporal inventory, ideally with independent training and testing subsets, is necessary before predictive performance can be claimed.
Finally, the earthquake-buffer analysis cannot establish seismic causation. No ground-motion, magnitude-depth attenuation, local site response or temporal matching was incorporated, and the use of nested buffers complicates distance interpretation. The entire product is a regional screening layer. It is unsuitable for parcel-level stability decisions, engineering design or forecasting without field-based geotechnical evidence.

## 6.0 Conclusions

This study developed a GIS-MCDA framework for screening landslide risk in Segamat by combining nine physical susceptibility indicators, ten exposure indicators and six vulnerability indicators. The physical component identified eastern and south-eastern Segamat as the principal zone of elevated susceptibility, reflecting the combined influence of slope, rainfall, lithology, lineaments and drainage proximity. Exposure was concentrated around settlements and services, while vulnerability increased where dependent population groups and limited access to emergency or health facilities coincided. Their multiplicative integration highlighted priority clusters around Kampung Abdullah and Taman Tan Leng Ann.

The earthquake-buffer analysis adds useful context but not causal attribution. Moderate-to-very-high susceptibility occupied 53.3%, 46.0% and 51.7% of the nested 5, 15 and 25 km buffers. The non-monotonic pattern, absence of a ground-motion layer and lack of time-matched landslide data mean that these values describe spatial co-location only. The current evidence does not justify labelling the mapped slopes as earthquake-induced landslide zones.

The principal value of the output is prioritisation. It can direct inventory building, field reconnaissance, geotechnical investigation, development review, drainage maintenance and community preparedness. Future work should document all dataset editions and AHP matrices, test weight and model-form sensitivity, replace coarse rainfall inputs with locally resolved observations, and validate the map against a systematic multi-event landslide inventory. Incorporating event-specific rainfall and ground motion would then allow the relative screening model to evolve towards a more defensible multi-hazard assessment.

**Acknowledgement:** The author gratefully acknowledges Universiti Sains Malaysia for supporting the research. The author also thanks the organisations that provide the geospatial datasets used in the analysis.

**Conflicts of Interest:** The authors declare no conflict of interest in this study

**Data Availability:** The source datasets are available from the organisations identified in Table 1, subject to their respective licences and terms of use. The derived GIS layers may be made available by the corresponding author on reasonable request. Exact editions or acquisition dates for several source layers were not recorded in the underlying research documentation.

**Ethical approval:** As the study is based on secondary data available in the public domain for research, no ethical approval was required from any institutional review board (IRB).

**Funding:** This research received no specific grant from any funding agency in the public, commercial or not-for-profit sectors.

**Author contributions:** Conceptualisation: Zhang Yibo and Mohd Amirul Mahamud; Methodology: Zhang Yibo, Ismail Ahmad Abir, and Mohd Amirul Mahamud; Literature search: Zhang Yibo and Ismail Ahmad Abir; Data collection: Zhang Yibo and Ismail Ahmad Abir; Data analysis: Zhang Yibo; Writing – original draft: Zhang Yibo; Writing – review and editing: Ismail Ahmad Abir and Mohd Amirul Mahamud; Critical review: Ismail Ahmad Abir and Mohd Amirul Mahamud; Supervision: Mohd Amirul Mahamud.

## References

Birkmann, J. (Ed.). (2013). Measuring vulnerability to natural hazards: Towards disaster resilient societies (2nd ed.). United Nations University Press.

Chigira, M., Wu, X., Inokuchi, T., & Wang, G. (2010). Landslides induced by the 2008 Wenchuan earthquake, Sichuan, China. *Geomorphology, 118*(3-4), 225-238. https://doi.org/10.1016/j.geomorph.2010.01.003

Crozier, M. J. (2010). Deciphering the effect of climate change on landslide activity: A review. *Geomorphology, 124*(3-4), 260-267. https://doi.org/10.1016/j.geomorph.2010.04.009

Dai, F. C., Xu, C., Yao, X., Xu, L., Tu, X., & Gong, Q. (2011). Spatial distribution of landslides triggered by the 2008 Wenchuan earthquake, China. *Journal of Asian Earth Sciences, 40*(4), 883-895. https://doi.org/10.1016/j.jseaes.2010.04.010

Farr, T. G., Rosen, P. A., Caro, E., Crippen, R., Duren, R., Hensley, S., Kobrick, M., Paller, M., Rodriguez, E., Roth, L., Seal, D., Shaffer, S., Shimada, J., Umland, J., Werner, M., Oskin, M., Burbank, D., & Alsdorf, D. (2007). The Shuttle Radar Topography Mission. *Reviews of Geophysics, 45*(2), RG2004. https://doi.org/10.1029/2005RG000183

Fell, R., Corominas, J., Bonnard, C., Cascini, L., Leroi, E., & Savage, W. Z. (2008). Guidelines for landslide susceptibility, hazard and risk zoning for land-use planning. *Engineering Geology, 102*(3-4), 99-111. https://doi.org/10.1016/j.enggeo.2008.03.022

Harris, I., Osborn, T. J., Jones, P., & Lister, D. (2020). Version 4 of the CRU TS monthly high-resolution gridded multivariate climate dataset. *Scientific Data, 7*, 109. https://doi.org/10.1038/s41597-020-0453-3

Keefer, D. K. (1984). Landslides caused by earthquakes. *Geological Society of America Bulletin, 95*(4), 406-421. https://doi.org/10.1130/0016-7606(1984)95%3C406:LCBE%3E2.0.CO;2

Lee, S., & Pradhan, B. (2007). Landslide hazard mapping at Selangor, Malaysia using frequency ratio and logistic regression models. *Landslides, 4*(1), 33-41. https://doi.org/10.1007/s10346-006-0047-y

Malaysian Meteorological Department. (2025, August 24). Earthquake information: Segamat, Johor, magnitude 4.1 [Seismic bulletin]. https://mygempa.met.gov.my/

Malczewski, J. (2006). GIS-based multicriteria decision analysis: A survey of the literature. *International Journal of Geographical Information Science, 20*(7), 703-726. https://doi.org/10.1080/13658810600661508

E-ISSN: 2948-5231
Article
Journal of Asian Geography, 2026, Volume 5 (Issue 2), 25-33
https://doi.org/10.36777/jag2026.5.2.3


Martin, S. S., Wang, Y., Muzli, M., & Wei, S. (2020). The 1922 Peninsula Malaysia earthquakes: Rare intraplate seismicity within the Sundaland block in Southeast Asia. *Seismological Research Letters, 91*(5), 2531-2545. https://doi.org/10.1785/0220200052

Nazaruddin, D. A., & Duerrast, H. (2021). Intraplate earthquake occurrence and distribution in Peninsular Malaysia over the past 100 years. *SN Applied Sciences, 3*, 607. https://doi.org/10.1007/s42452-021-04686-2

OpenStreetMap contributors. (2025). *OpenStreetMap data for Segamat, Johor* [Data set]. https://www.openstreetmap.org

Reichenbach, P., Rossi, M., Malamud, B. D., Mihir, M., & Guzzetti, F. (2018). A review of statistically-based landslide susceptibility models. *Earth-Science Reviews, 180*, 60-91. https://doi.org/10.1016/j.earscirev.2018.03.001

Saaty, T. L. (1980). *The analytic hierarchy process: Planning, priority setting, resource allocation.* McGraw-Hill.

Shahabi, H., & Hashim, M. (2015). Landslide susceptibility mapping using GIS-based statistical models and remote sensing data in tropical environment. *Scientific Reports, 5*, 9899. https://doi.org/10.1038/srep09899

Simons, W. J. F., Socquet, A., Vigny, C., Ambrosius, B. A. C., Haji Abu, S., Promthong, C., Subarya, C., Sarsito, D. A., Matheussen, S., Morgan, P., & Spakman, W. (2007). A decade of GPS in Southeast Asia: Resolving Sundaland motion and boundaries. *Journal of Geophysical Research: Solid Earth, 112*(B6), B06420. https://doi.org/10.1029/2005JB003868

Tatem, A. J. (2017). WorldPop, open data for spatial demography. *Scientific Data, 4*, 170004. https://doi.org/10.1038/sdata.2017.4

Van Westen, C. J., Van Asch, T. W. J., & Soeters, R. (2006). Landslide hazard and risk zonation—Why is it still so difficult? Bulletin of Engineering Geology and the Environment, 65(2), 167-184. https://doi.org/10.1007/s10064-005-0023-0

Zanaga, D., Van De Kerchove, R., Daems, D., De Keersmaecker, W., Brockmann, C., Kirches, G., Wevers, J., Cartus, O., Santoro, M., Fritz, S., Lesiv, M., Herold, M., Tsendbazar, N. E., Xu, P., Ramoino, F., & Arino, O. (2022). *ESA WorldCover 10 m 2021 v200* [Data set]. Zenodo. https://doi.org/10.5281/zenodo.7254221